Electron emission and electron transfer processes in proton-naphthalene collisions at intermediate velocities

P. M. Mishra,[1] J. Rajput,[2] C. P. Safvan,[3] S. Vig,[4] and U. Kadhane[1,*]

[1]*Department of Physics, Indian Institute of Space Science and Technology, Trivandrum-695 547, India*

[2]*Department of Physics and Astrophysics, University of Delhi, Delhi-110 007, India*

[3]*Inter-University Accelerator Centre, Aruna Asaf Ali Marg, New Delhi-110 067, India*

[4]*Department of Earth and Space Science, Indian Institute of Space Science and Technology, Trivandrum-695 547, India*

(Received 18 August 2013; published 15 November 2013)

We investigate the fragmentation and ionization of naphthalene by protons at intermediate velocities (between 1.41 and 2.68 a.u.). Relative cross sections for electron capture (EC), electron emission (EE), and capture ionization are measured. The EC cross sections decrease rapidly over the energy range under consideration (50–150 keV) and are lower than EE cross sections. The EE cross sections, on the other hand, change very slowly in this energy range. The energetics of interactions is quantified by comparing the mass spectra with the photodissociation breakdown curves from literature. In the case of single capture, resonant electron transfer to $n = 1$ state in H^+ is seen to dominate the interaction but is shown to be accompanied by a small amount of electronic energy loss. In the EE mode, two mechanisms are shown to be active in the collision process: large impact parameter plasmon excitation mode, and closer encounters with higher amounts of electronic energy loss.

DOI: 10.1103/PhysRevA.88.052707 PACS number(s): 34.50.Gb, 34.50.Bw, 34.70.+e, 36.40.Gk

I. INTRODUCTION

Ion-molecule collisions at intermediate velocities are relatively complex due to competing magnitudes of ionization and electron transfer cross section. Collective or plasmon excitation in some molecules plays a significant role in these interactions, particularly in the ionization process, as shown by the photoionization studies [1,2]. Isolating these contributions in the ion-molecule collision process is a challenging task due to the broad energy deposition. Therefore postcollision analysis of energy deposited in the target molecule in this velocity regime can shed light on the understanding of such excitations. Polycyclic aromatic hydrocarbon (PAH) is a large family of molecules which is known to have such collective excitation [1]. But this aspect has remained unexplored in collisions with charged particle radiation. The importance of the PAHs in terrestrial [3–7] and astronomical environments [8] has resulted in intense study of their structure and dynamics in the last couple of decades. PAHs, though complex, demonstrate unusual resilience in the presence of harsh radiation. It is instructive to study the interaction of intermediate velocity (∼1 a.u.) protons with small PAH molecules as it will enhance our understanding of the way low-energy cosmic ray protons interact with PAHs in the interstellar medium (ISM), thus providing inputs to various models. Since typical ionization cross sections of PAHs peak at ∼10 keV for proton projectiles and ∼50 eV for electrons, our understanding of low-energy collision processes, therefore, becomes important [9]. While laboratory measurements of the interaction of PAHs with electromagnetic radiation have been investigated numerous times, studies relating to interaction with ions are relatively few. These include ionization and fragmentation of naphthalene by electron impact [10,11]. Due to broader energy deposition distribution in ion-PAH collision, they are difficult to investigate in terms of rate constants for various dissociative channels [12–16]. Recently, slow charge particle (velocity $v \ll 1$ a.u.) collisions with PAHs and their clusters leading to multiple ionization and fragmentation has been studied [16–20]. Postma *et al*. [16] have emphasized the importance of collisions at relatively higher velocities (∼1 a.u. or more) in the reverse shock of the early stage of supernova remnants. However, to the best of our knowledge, no laboratory measurements in this velocity regime have been reported.

It is expected that collisional excitation due to charge particle for molecules bearing delocalized electrons are influenced by a multiparticle excitation process such as plasmon excitation characterized by a large oscillator strength [1,21]. One of the prominent modes of excitation in PAHs is the collective oscillation of charges [1,21,22]. There have been several detailed investigations of such plasmon resonance excitations in the case of fullerenes and their derivatives [2,23,24]. This characteristic excitation ranges in energy from 16 to 25 eV as one goes from planar PAHs to fullerenes and then bulk graphite [1]. Due to its large excitation cross section, it is been shown to dominate single and even double ionization of fullerenes in ion-fullerene collisions [24]. It is important to note that the influence of this plasmon resonance excitation in ion-PAH collisions, other than C_{60}, has been insufficiently investigated. An examination of this process will, therefore, help in understanding the energetics of the collision process as well as the postcollisional relaxation mechanisms. It is to be noticed that the plasmon resonance peak for PAHs is at ∼17 eV [1] and the onset of H loss and C_2H_2 loss dissociation channels is at ∼15 eV for naphthalene [25]. Therefore, an examination of these dissociation channels in ion-naphthalene collisions can explore the extent of influence of the plasmon excitation in these processes. In addition, it will help in isolating two different modes of interactions, namely (a) plasmon excitation causing ionization and H or C_2H_2 loss, and (b) multifragmentation of naphthalene.

In view of the above points the present study dealing with ion-PAH collisions helps in understanding the physics behind

*umeshk@iist.ac.in

the ionization and capture process by isolating them on the basis of internal energy deposited into the molecule within the intermediate velocity regime. Though the PAH family is shown to have plasmon excitation [1], due to the possibility of low-energy evaporative pathways, such measurements on PAHs are complex. The present work lies in this velocity regime (1.41–2.68 a.u.; EC mode is restricted to up to 2.45 a.u.) where ionization, fragmentation, and their dependence on projectile energy are investigated with the help of relative cross sections measured in electron capture (EC) and electron emission (EE) mode, while the capture ionization (CI) cross sections were derived using EE and EC mode data in coincidence. Multiple ionization events were analyzed using the yield of the respective ionization peaks in the presence or absence of electron and neutralized projectile coincidence. By neglecting the double-capture process, these yields were used to extract the relative cross sections for ionization due to pure electron emission as well as by single capture along with electron emission. The following pathways are considered:

for EC mode :
$$H^+ + C_{10}H_8 \rightarrow H^o + ne^- + \text{(parent ion or fragment ion)},$$
for EE mode :
$$H^+ + C_{10}H_8 \rightarrow H^+/H^o + me^- + \text{(parent ion or fragment ion)},$$

where $n \geqslant 0$ and $m \geqslant 1$.

Upon excitation, PAHs and their cations typically undergo deexcitation either by emitting IR radiation or by H loss. The other favorable dissociation channel is C_2H_2 loss. The H_2 loss starts dominating if the internal energy deposited in the molecule increases [15,26–28]. These observations are supported theoretically by the Rice, Ramsperger, and Kassel (hereafter RRK) model which has been used to interpret the loss channels by estimating their rate constants [28] and thermo-photo-dissociation rates [29]. Multiply charged PAH ions may decay by emitting H^+ and $C_2H_2{}^+$ ions [19,27]. Vuong *et al*. find that the PAHs tend to be dehydrogenated in diffuse cloud environments where the hydrogen density is about 0.1–100 cm^{-3} and the temperature is ∼100 K [30]. Larger PAH molecules (having more than 50 carbon atoms) have more degrees of freedom for storing the excess energy deposited by UV absorption. Hence, they are less prone to dehydrogenation even in low-H-density regions of the ISM [30]. In the astronomical context, it is widely believed that these molecules are responsible for several unidentified absorption and emission bands in the optical and infrared region, respectively [31–36]. The investigation into the behavior of neutral and ionic PAHs with charged particles and radiation is crucial for a variety of reasons. They contribute to the heating and ionic balance of the ISM [37]. Further, they act as catalysts in the formation of molecular hydrogen in low-UV-flux regions where they can remain in hydrogenated form for longer time scales. This has been experimentally proven for coronene [38].

In the present study, we have explored the energy dissipation mechanisms related to H, $2H/H_2$, and C_2H_2 loss and consequently, the stability of PAHs under proton impact at different energies. Further, such an experiment has allowed us to probe the competition between ion-induced violent multifragmentation process and stable multiply charged intact molecular ion formation in different regimes of proton projectile energy. It is known that an electron removal from the target due to the capture process transfers less excitation energy to the target molecule as compared to direct ionization process [39]. Several proton impact studies have been carried out to understand these interactions for many atomic [40–42] and biologically relevant molecular targets [43–48] at energies similar to those used in the present experiment.

We have compared our results on the electron emission and capture processes with those mentioned above, i.e., fullerenes and nucleobases (due to similarity in composition, structure, and degrees of freedom). This is due to lack of data on PAHs in the present energy range. Lekadir *et al*. [49] have carried out Monte Carlo calculations on five nucelobases and have shown that for proton projectile in the range from 10 keV to 10 MeV, single-capture as well as single-ionization cross sections show very minor differences [49]. In spite of having large differences in the total number of electrons and binding energy values, the similarity in ionization cross sections is an indication that, in the present velocity regime, the total electron density and density distribution are vital in determining various electron loss processes. Identical observations are made for single-capture cross sections. Similar conclusions have been drawn from experimental measurements on these nucleobases in the present energy range [42].

II. EXPERIMENTAL DETAILS

The experiment was carried out at the Low Energy Ion Beam Facility, Inter-University Accelerator Centre, New Delhi, using an electron cyclotron resonance ion source mounted on a high-voltage deck. Proton beams of energy between 50 and 180 keV were made to collide with a naphthalene target. Napthalene was effusing from a needle placed perpendicular to the projectile beam path in the collision chamber. The chamber pressure was 5×10^{-7} Torr during the experiment. The naphthalene sample was obtained from Sigma-Aldrich with 98% purity. Since the vapor pressure of naphthalene is 0.0817 Torr, no heating was required for evaporation. There was no contamination seen in the time-of-flight (TOF) spectrum due to impurities in the sample.

A linear two-field TOF mass spectrometer (TOFMS) with a position-sensitive microchannel plate detector was used to detect the recoiled naphthalene ions after interaction with the proton beam. The electrons ejected in the process were extracted in a direction opposite the TOFMS and detected by a channeltron (C1). The neutralized projectile beam (as a result of electron capture process) was detected by a second channeltron (C2) placed in the path of the beam at a distance 1.5 m from the collision chamber. Postcollision, the charged projectiles were deflected away from this detector using an electrostatic deflector. The start triggers for electron emission (EE) and electron capture (EC) modes were taken from the ejected electrons and neutralized projectile beam, respectively. The stop signal was taken from the microchannel plate detector. Multicoincidence measurements were carried out in both EE and EC modes by a CAMAC based multihit data acquisition system (DAQ) employing LeCroy time-to-digital converter (model 3377 TDC). The detailed layout of the experimental setup and DAQ is described elsewhere [50].

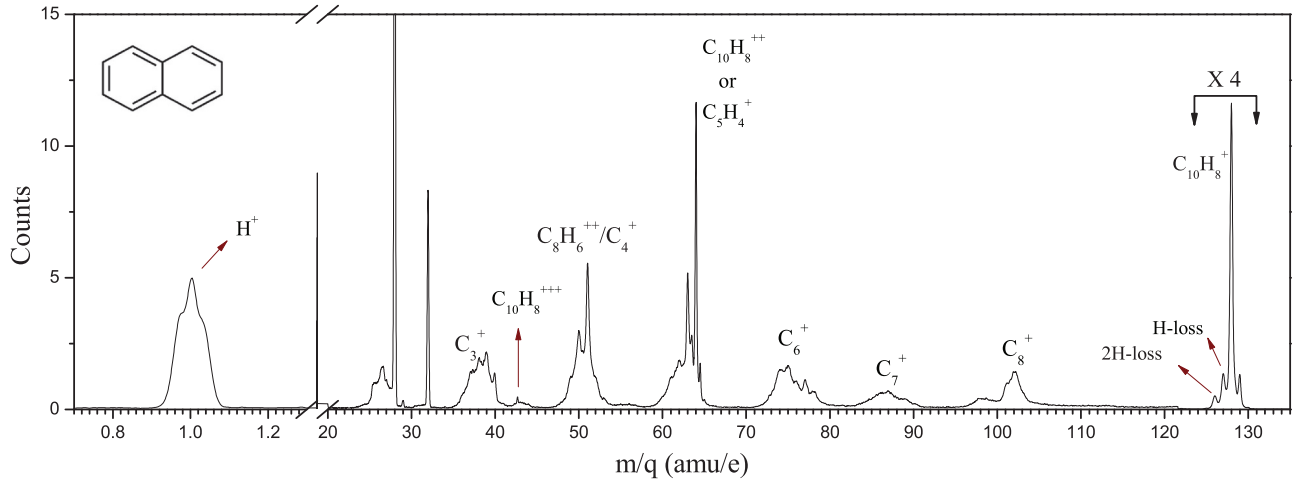

FIG. 1. (Color online) Mass spectrum for 100-keV proton projectile beam in electron capture mode showing H, $2H/H_2$, C_2H_2 loss from naphthalene ion and fragment ions.

The mass spectra were isolated according to the detection mode in order to extract the relative experimental cross sections by appropriately correcting for the ion, electron, and neutralized projectile detection efficiencies. The ion detection efficiency for the microchannel plate detector has been obtained using an empirical model reported in the literature [51].

The relative cross sections are normalized to the electron (8%) and neutralized projectile beam detection efficiency (5%–20%, depending on beam tuning condition) in EE and EC modes, respectively. Since we neglect contributions due to double capture, the double ionization of the target can occur, either by (a) transfer of one electron to projectile as well as emission of one electron, or by (b) two-electron emission. Hence, by using yields of dication with and without electron detection in EC mode, we have been able to determine the electron detection efficiency. The possibility of multiple electron detection (along with neutralized projectile detection probability in relevant cases) has been considered in efficiency correction for double- and higher-ionization relative cross sections. The projectile detection efficiency as well as the target thickness and total beam flux were obtained for each projectile energy using the present experimental yields and previously published N_2 ionization and capture cross sections [52]. In this process it is assumed that the target density was in constant proportion to the N_2 and O_2 gas. This has been independently checked by comparing the yield ratios under identical experimental conditions at different times during the experiment. The TOF mass resolution ($\Delta M/M$) in the case of EC mode was better than 1/128. However, in EE mode the resolution was poor due to a slightly distorted start signal from the channeltron C1.

In the absence of absolute target density values, only the relative values of all cross sections for ionization, dissociation, and multifragmentation channels could be estimated. The constant of proportionality, needed to relate all the relative cross sections to their respective absolute cross sections, is a single common factor for all the measurements. The overall target density fluctuations as well as errors in the efficiency are within 10%–20% of the value in all cases except triple ionization where poor statistics lead to ∼30% error. In our analysis, we have assumed that double capture is negligible.

III. DISCUSSION

A. Single and multiple ionization

The mass spectrum for 100 keV proton impact on naphthalene in EC mode is shown in Fig. 1. Here, the multiply ionized parent molecule M^{q+} (up to $q = 3$), the loss of H, $2H/H_2$, C_2H_2, and other fragmentation channels is clearly visible. Note the peaks at m/q of 129, 128, 127, and 126. These correspond to (i) naphthalene isotopic peak with one ^{13}C, (ii) naphthalene with all ^{12}C, (iii) H loss, and (iv) 2H or H_2 loss, respectively. The isotopic ratios for mass 128 and 129 are found to be consistent within the expected value of 11%. Single ionization is observed to be the most prominent channel followed by double ionization. In the dication region, the mass spectrum shows a composite peak with a sharp narrow peak overriding a broad feature. The peak at m/q of 64 can arise either due to a singly charged half mass peak or due to a doubly charged intact molecule. This ambiguity was resolved by comparing the area of the isotope peak at 64.5 mass (which gave the correct isotopic ratio) with the area of sharp peak at 64 alone, allowing us to conclude that the sharp peak structure is due to the dication species. The broad peak is likely to be due to the violent fragmentation of multiply charged species leading to a singly charged $m/q \leqslant 64$ mass fragment. Ionization of naphthalene up to charge state 3+ is observed but the intensity is low compared to multifragmentation channels.

The case of double ionization is conspicuous in the sense that this double-ionization yield is much larger than the $2H/H_2$ and C_2H_2 loss. This is in contrast with collision of nucleobases with protons (in the same energy range) where the fragmentation channels dominate and multiple ionization is negligible [44]. Considering that molecules such as adenine and guanine are of the same mass range as naphthalene and have similar elemental composition, the electronic energy loss is also expected to be similar. Hence, we see that there is a clear difference in the ionization mechanism in the two cases. Large delocalization due to conjugation gives PAHs the

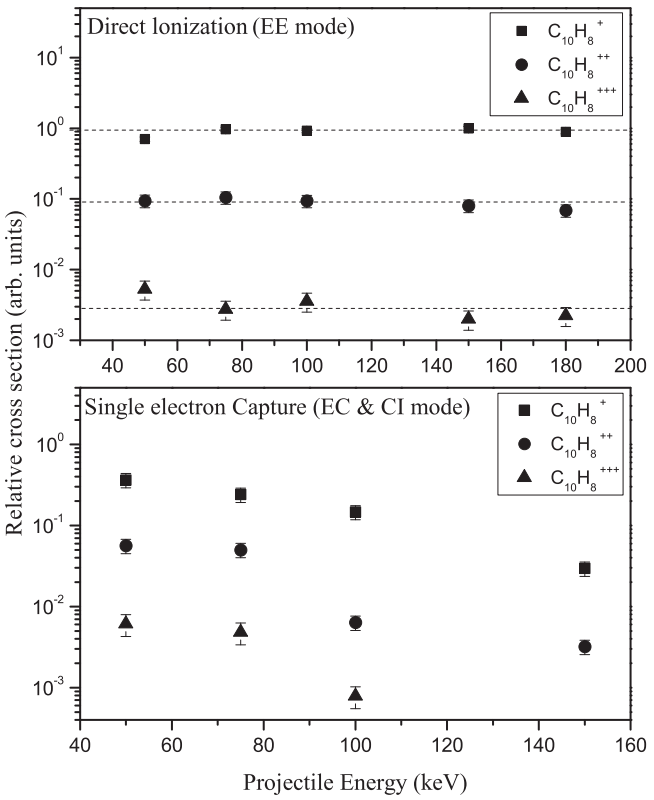

FIG. 2. Relative cross sections as a function of proton projectile energy for singly, doubly, triply ionized naphthalene in EE (top) and EC (bottom) mode. The dashed line is a guide to eye.

ability to accommodate excess charge without dissociation. This is well known in the case of C_{60} where metastable fullerenes with charge state up to 12+ have been detected experimentally [53]. The presence of heteroatoms in the case of nucleobases may cause reduction in such delocalization, thus reducing the threshold energy for fragmentation compared to multiple ionization.

There are a few prominent differences between the mass spectra obtained under EE and EC modes at the same energy. A detailed discussion is carried out in later sections. For these modes, after normalizing to their respective single-ionization yields as well as correcting for neutralized projectile and electron detection efficiencies, we find that the double- and triple-ionization yields are higher in EE than in EC mode as shown in Fig. 2. Also, the C_2H_2 and $2H/H_2$ evaporation from dication is lower for EE than for EC mode. This indicates that in EE mode, the production of dication involves a lower amount of excess energy than in the case of EC. Consequently, the internal heating is lower, leading to less evaporation. The fragmentation yields, on the other hand, are much larger in EE mode. This is explained on the basis of two different modes of energy transfer (see later). Finally, due to poor resolution in EE mode, peak fits were not reliable in the single-ionization region. Therefore, qualitative conclusions regarding H loss and H_2 loss are drawn from EC mode data and are assumed to be valid for EE mode as well. In both cases the C_2H_2 loss yields were obtained for the sharp peak at $m/q = 102$.

Single- and double-ionization cross sections in EE mode are observed to be almost constant within error bars, where as the corresponding cross sections in the EC and CI modes decrease with impact energy by about an order of magnitude (Fig. 2). Several studies have shown that for collisions of proton with diatomic molecules [54], linear hydrocarbons [42], and nucleobases [44,49], the ionization cross sections in the present projectile velocity range decrease by a factor of 3. However, for C_{60} the cross sections increase slowly with energy [55], approaching a constant value for energies larger than 100 keV. On the other hand capture cross sections show a drastic decrease with projectile velocity, as seen in all the above stated cases (except C_{60} where the relevant numbers are not available for comparison) [42,45,49,54,56]. Using the expression for calculating single-ionization cross sections given by Stolterfoth *et al.* [57] and binding energy [obtained from density functional theory (DFT) calculation] values, we calculate single-ionization cross sections for naphthalene which also show a drop by a factor of 3. These observations, together with the fact that plasmon excitation plays a major role in single ionization of PAHs, [1,22] indicate that plasmon resonance excitation could be the principal single-ionization channel here (similar to the case of C_{60}). Further, this channel is known to have weak velocity dependence for C_{60}, particularly in the present energy range [24,55].

Single-electron capture cross sections are found to decrease with increase in projectile velocity ($\sim v^{-4}$). This scaling is much slower than that from the Bohr-Lindhard model [58] where the cross sections should drop approximately as v^{-7} for sufficiently fast projectiles. It is important to note that such models assume the target to be either pointlike or spherically symmetric. However, it is difficult to adopt such formalism here for the following reason. In the velocity regime under consideration, the capture distance is expected to be small, ~11 a.u. for naphthalene as per Coulomb barrier estimate [59]. This is close to the actual molecular size of naphthalene, ~11.71 a.u. [60]. Since naphthalene is planar, the assumptions about the target (pointlike or spherically symmetric) do not strictly apply. Recently, Forsberg *et al.* have attempted to make a Coulomb barrier model for large planar PAHs [61]. However, this can only be applied in relatively simple cases, unlike naphthalene. Moreover, as shown in a later section, the active electron in the transfer process is from an inner valence shell. Therefore the velocities in the present regime may not be high enough for Bohr-Lindhard scaling to be applicable.

Figure 3 shows the singly charged naphthalene ions formed by EC process as a percentage of the total number of singly charged naphthalene ions produced in the present study, i.e., $[EC/(EC + EE)] \times 100$ along with published values for other molecular targets: O_2, CH_4, CO_2, and uracil ($C_4H_4N_2O_2$) [44,48,52,56,62]. Note that, irrespective of size, composition, and type of molecular target, the EC cross section decreases with increase in impact energy. Naphthalene also follows this trend fairly well. The highest occupied molecular orbital (HOMO) energy for such a variety of examples is different and the capture probability of the HOMO electron should also vary considerably. But the observed similarity in the capture fraction indicates that the HOMO energy is not an appropriate parameter governing the contribution of EC and EE processes in proton collision with molecules.

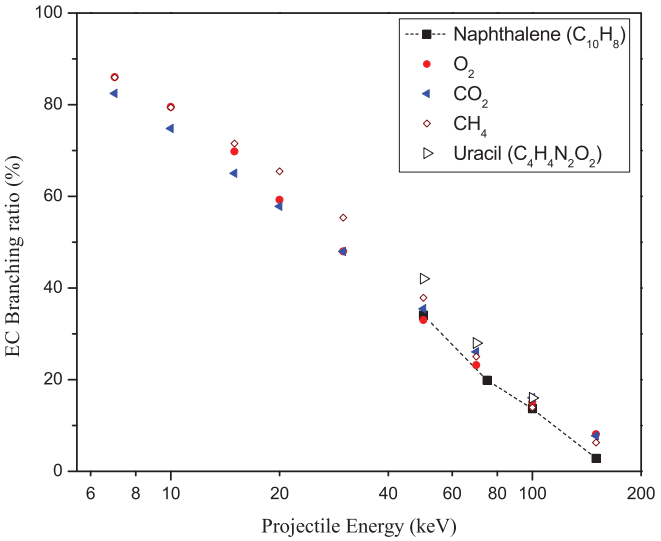

FIG. 3. (Color online) Capture fraction (in percentage) for various molecules in collision with protons.

B. H loss, $2H/H_2$ loss, and C_2H_2 loss

A number of evaporative channels are observed in the mass spectra. It is well known that H loss is a prominent evaporation mechanism by which the molecular ion of PAH can reduce its internal energy [25,28]. In the case of 2H or H_2 loss, it is not possible to distinguish between the two channels, i.e., whether the loss of H was sequential or simultaneous (in the form of molecular hydrogen). The latter is energetically favored but less probable at lower internal energy [27,63]. Rousseau *et al.* [64] have shown that when 11.25-keV He^+ ions collide with anthracene molecules, $2H/H_2$ loss is much larger than H loss for single ionization. On the other hand, collision with Xe^{10+} beam at 360 keV produces anthracene ions with almost no $2H/H_2$ loss and the fraction of H loss is very small. He^+ collision is expected to cause single ionization at a much lower impact parameter than Xe^{10+} collision. Hence the former projectile will deposit more internal energy than the latter. Therefore, the dominance of 2H loss peak in He^+ collisions over H loss implies that this particular peak is not due to sequential H loss but a loss of molecular H_2. In other words, at lower internal energies, the sequential double H loss mechanism is effective and at higher internal energies it is the molecular H_2 loss mechanism. The trend is similar for coronene and pyrene [18]. In the present case, the average electronic stopping is considerably less than those with lower velocities of He^+ ions discussed above. Hence, the sequential loss of 2H is more likely than the loss of H_2.

For the deexcitation of PAHs, IR emission is expected to compete with other channels such as H, $2H/H_2$, or C_2H_2 loss at a decay rate of 10^2 s^{-1}. At higher decay rates, the dissociation channels dominate [65]. It has been shown, both experimentally and theoretically, that for naphthalene molecule at the appearance energy of the above-mentioned loss channels, the decay rates are 10^4 s^{-1} or more [28]. The measured appearance energies are 15.41, 15.60, and 15.50 eV for H, H_2, and C_2H_2 loss, respectively [28]. Considering that the ionization potential is 8.12 eV, the minimum internal energy required for the above-mentioned loss channels would be 7.40, 7.59, and 7.49 eV, respectively, with 0.11 eV average thermal energy, in order to be observed in our experimental TOF range (which requires a limiting decay rate of 10^5 s^{-1}). Further, we note that other higher mass dissociation channels have appearance energy values close to (within a few eV) the appearance energy of H, 2H, and C_2H_2 loss channels [66]. Therefore, at a higher internal energy, other dissociative channels will open up. This implies that the H, $2H/H_2$, and C_2H_2 loss mass spectra are sensitive to internal energy variation in our TOF range (10 μs). Consequently, any small change in the energy deposition close to the appearance energy will reflect in a large variation of H, $2H/H_2$, and C_2H_2 loss yields in comparison to single intact ionization. This argument is of vital importance in the forthcoming discussions.

These decays have been modeled for naphthalene as an Arrhenius type of decay by Gotkis *et al.* using photoionization data. They have derived activation barriers as 4.23 and 4.6 eV for H and C_2H_2 loss, respectively [25]. Ho *et al.* repeated these activation barrier measurements on naphthalene ions using two-photon absorption time-resolved photodissociation method and obtained values of 4.48 and 4.41 eV for H and C_2H_2 loss, respectively [67]. On the other hand, Jochims *et al.* [28] and Allain *et al.* [65] have followed a simpler RRK approach with bond activation energies of 2.8 and 2.9 eV for H and C_2H_2 loss, respectively. The calculations are expected to be applicable to both forms of naphthalene, neutral and cationic, with identical decay parameters [28]. Recently West *et al.* have considered a much larger number of channels and accurately determined the Arrhenius parameters for the statistical dissociation of naphthalene monocation [68]. To estimate the range of energy loss in the present case, we use the 0 K breakdown curves obtained by West *et al.* [68] which have a similar TOF time scale as in the present case. From these curves, we note that for the total energy deposition below 18 eV, C_2H_2 loss fraction is the same as H loss fraction. We find an analogous behavior for the EC mode, as shown in Fig. 4. In other words, most of the events leading to single-ionization deposit energy less than 18 eV in EC mode. On the other hand, EE mode shows 30% less yield of C_2H_2 compared to EC mode, implying that a significant fraction of collisions leading to single ionization involves energy deposition larger than 18 eV.

Holm *et al.* have shown that with increasing charge state, the loss of charged species becomes energetically more probable [27]. For naphthalene, it has been shown that for the charge state $q = 2$, the charged fragment evaporation becomes energetically comparable to neutral evaporation. The multicoincidence analysis in the present study shows that for H, $2H/H_2$ loss peaks, there are no detectable charged fragments in coincidence. However, we do observe a detectable but weak correlation channel between charge fragment of C_2H_2 loss in coincidence with $C_8H_6^+$ or more prominently with $C_8H_5^+$ fragment. This is discussed in detail elsewhere [69]. We, therefore, conclude that even for the doubly charged parent ion case, the charged fragment evaporation is not a favorable channel for naphthalene. As a result, the loss of H, $2H/H_2$, and C_2H_2 can be considered as loss through evaporation of neutrals, predominantly.

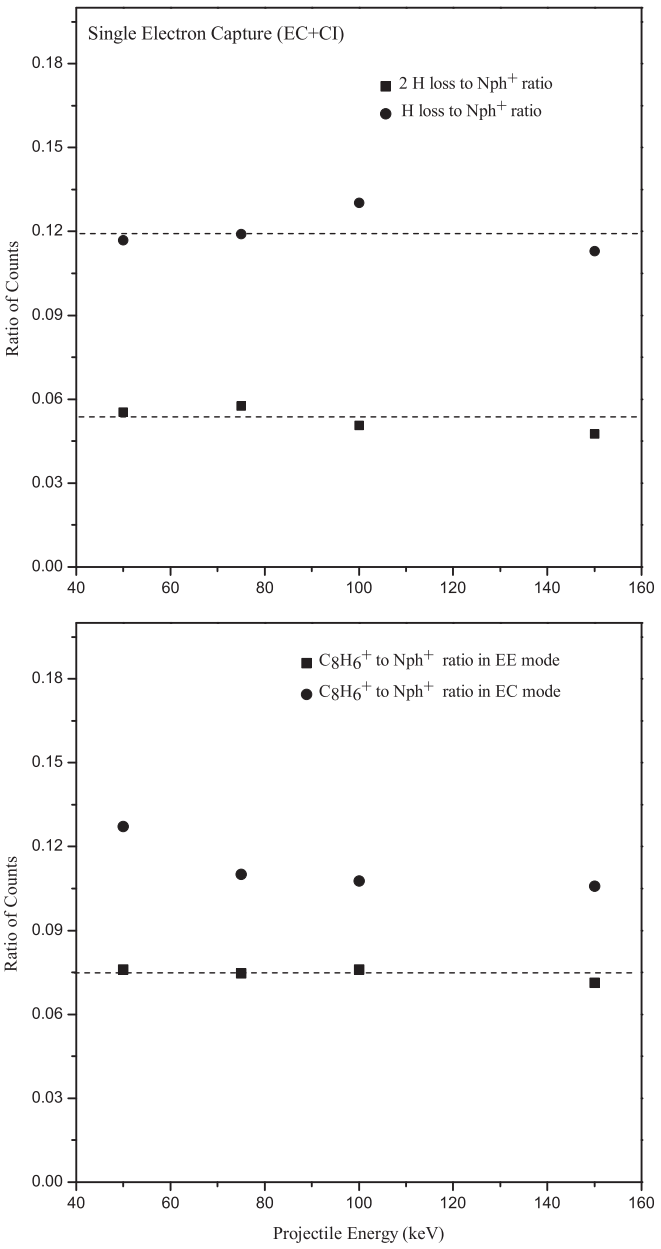

FIG. 4. Proportion of H and $2H/H_2$ loss with respect to intact naphthalene molecular ion in capture mode (top) and proportion of C_2H_2 loss with respect to intact naphthalene molecular ion in capture and ionization mode (bottom). The dashed lines represent constant values of ratio of counts.

In the double-ionization case, the loss of $2H/H_2$ dominates over H loss corroborating the fact that double ionization requires lower impact parameter collisions compared to single ionization. This leads to a higher amount of electronic energy loss. Also noteworthy is the observation that a large fraction of doubly charged naphthalene ions lose C_2H_2 giving rise to the sharp peak at m/q of 51. This peak is followed by another sharp peak corresponding to loss of $(C_2H_2 + H_2)$. These observations are in agreement with the results obtained for ion-anthracene collisions at lower energies [70]. The measurements with anthracene have shown that loss of C_2H_2 dominates for internal energy less than 13 eV while sequential loss of H is the dominant mechanism at internal energies higher than 13 eV [70]. These observations can be extrapolated to naphthalene considering the structural similarity. However, the lower degrees of freedom may lower the limiting values of the internal energy to less than 13 eV. Postma *et al*. have studied ion-anthracene collisions at lower energies using a reflectron TOF. Since a reflectron TOF compensates for the kinetic energy spread, it is not possible to distinguish if m/q of 51 is a singly or doubly charged fragment species [16]. However, in our case, a clear difference in the peak shape helps in the identification.

C. Multiple fragmentation

The fragments containing C_6, C_7, and C_8 are broad indicating their origin to be multiply charged naphthalene ion (Fig. 1). This is over and above the overall widths due to a variable number of H attached to such fragments. However, there are narrow features riding the broad peaks. These arise from the evaporation process of neutrals, e.g., one or two C_2H_2 fragments. This is also a prominent and well-studied channel for PAHs [27]. We, therefore, attribute the narrow features at m/q of 102 and 77 to the loss of C_2H_2 and $(C_2H_2 + C_2H_1)$, respectively. Further, the C_7 mass fragments show no sharp features due to lack of evaporation or cold dissociative channel such as acetylene loss in the case of C_8.

We observe prominent fragmentation peaks at m/q positions of $C_nH_m{}^+$ ($n = 2, 3, 4, 5, 6, 7, 8$ and $m \geqslant 0$). Fragments with single C atom or with nine C atoms were negligibly small. All the fragmentation peaks were sufficiently broad to have substantial overlap with the adjacent mass value. The overall observation is that for every C cluster fragment, i.e., $C_nH_m{}^+$, the yield is maximum for $m = 2$ or 3. A prominently sharp peak at m/q of 26.5 indicates doubly charged C_4H_5 fragment. Low impact parameter collisions lead to a substantial amount of energy transfer to the target. This can cause multiple ionization followed by Coulomb explosion, giving rise to fragment ions with high kinetic energies. Fragmentation of this type has been observed for proton-anthracene interaction by Postma *et al*. [16]. They have estimated an average energy loss of ~58 eV for protons with energy 15 keV, leading to multifragmentation. Their model shows a linear variation of average energy loss with projectile velocity. Although the model is for lower projectile velocities (<1 a.u.), we have used it in our case (projectile velocity of 1.41 a.u.) in order to get an approximate value of energy loss. This corresponds to ~116 eV. We have also assumed that the maximum cross section is offered by the molecule with its plane perpendicular to the beam.

D. Resonant electron transfer

Figure 5 shows the mass spectra of all the studied projectile velocities in EE and EC modes normalized with parent single-ionization peak area. In the EC mode, the change in cross section across energy is about an order of magnitude. However, on normalization with respect to the parent single-ionization peak area for all the projectile energies (50–150 keV), the evaporation as well as multifragmentation channels overlap (Fig. 5). It is, therefore, evident that the projectile is depositing

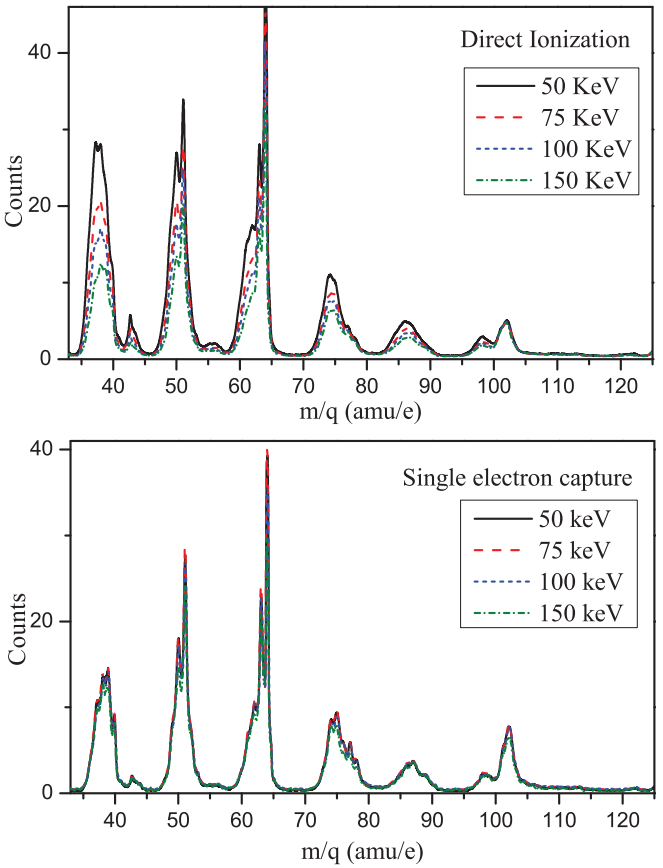

FIG. 5. (Color online) Mass spectra of EE mode (top) and EC mode (bottom) normalized to parent single-ionization peak area for different proton projectile energies.

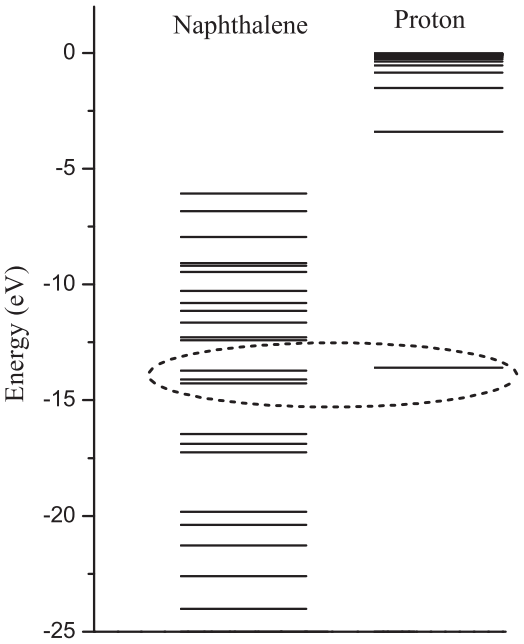

FIG. 6. Energy level diagram for naphthalene target (obtained using DFT at B3LYP/6-311G($2d,p$) level) and proton projectile.

the same amount of energy in EC mode across the entire velocity range. We explain these observations on the basis of resonant or quasiresonant electron transfer from target to projectile accompanied by electronic stopping [16,71]. As mentioned earlier, singly ionizing events in EC mode lead to total energy deposition <18 eV. We have performed structure calculations for naphthalene using DFT at B3LYP/6-311G ($2d,p$) level with the help of GAUSSIAN 03 [72]. The molecular orbitals are calculated and their respective symmetries and binding energies were assigned.

We find that five molecular orbitals (with symmetries b_{2u}, b_{3g}, a_g, b_{1u}, and a_g) with binding energies between 12 and 14 eV can possibly match the $n = 1$ bound state of the proton-electron system. A plot comparing the energy levels of the target (naphthalene) and projectile (proton) is shown in Fig. 6. From this figure, it is clear that the rearrangement following the capture will cause the internal energy to be elevated by about 6 eV leading to the likely evaporation of H, H_2, or C_2H_2. Since energy deposition for the resonant transfer is constant, the internal energy distribution is also constant. Comparing the relative yields of intact ions as well as H, H_2, and C_2H_2 loss species with the photoionization breakdown curves by West *et al.* [68], we observe that the internal energy after capture should be ∼7.5 eV. This is in agreement with the internal energy values of ∼7.1 eV obtained by Gotkis *et al.* [25]. However, the measurements by Ho *et al.* [67] using two-photon excitation of naphthalene cation indicate that C_2H_2 loss is higher than H loss at deposition energy of 7.1 eV. Therefore, to have the observed ratios of relative yields of the evaporation channels, the internal energy ought to be more than 8 eV. This implies that the capture process is accompanied by a considerable amount of electronic energy loss, ∼2 eV. The majority of events in EC mode therefore correspond to an energy loss that is limited to 14–16 eV, consistent with the upper limit of 18 eV.

E. The energetics of electron emission process

In the case of direct ionization mechanism (i.e., EE mode) the evaporation process of C_2H_2 shows no dependence on impact energy (Fig. 4). Due to poor resolution, the yields of H and 2H loss channels could not be plot separately. The single-ionization peaks (which includes the H and 2H loss channels as well as an isotope peak) for the entire energy range under consideration overlap exactly, demonstrating the independence of projectile velocity in these channels. As these channels are very sensitive to energy deposition, we are inclined to take the view that the energy deposition in EE mode should also be constant over the present velocity range, analogous to EC mode. However, from the fragmentation yields, it appears that the energy loss by the projectile varies significantly (Fig. 5). The fragmentation yields decrease considerably with increase in projectile velocity. At 150 keV (highest projectile velocity), we find that the fragmentation yields approach the respective values in EC mode. Therefore, we anticipate a substantial variation in the energy deposition and consequently, in the overall decay rates. The ratio of multifragmentation peak areas is observed to vary by almost an order of magnitude in a few cases, e.g., C_2^+.

Although the C_2H_2 yields are constant across the energy range investigated here, the yields for EE mode are ∼30% lower than the EC mode when the corresponding intact parent single-ionization peak areas are normalized (see Fig. 4). These lower C_2H_2 yields in EE mode, when considered with the breakdown curves by West *et al*., imply that for singly ionizing events, the energy loss distribution can be higher than 18 eV [68]. However, it cannot be significantly higher lest H loss yield falls below 2H loss yields. It can, therefore, be concluded that energy loss from the projectile to the naphthalene target molecule occurs in two ways. First, there is a large impact parameter regime in which energy of ∼16–18 eV is deposited which leads to single ionization, sometimes followed by evaporation. The second process involves a lower impact parameter collision process. Here, the projectile deposits higher energy into the target causing violent multifragmentation with substantial projectile velocity dependence.

Plasmon resonance plays a major role in the photoionization of PAHs [1,22] and is known to dominate the cross section for single ionization in the energy range 13–19 eV, with a peak at ∼17 eV (for planar PAHs). This collective resonance (at ∼20 eV for fullerenes) also causes single and double ionization of C_{60} in the ion-C_{60} collision process and shows very weak projectile velocity dependence [24]. In the present experiment, we observe that the ionization as well as evaporation processes are independent of projectile velocity. In addition, comparison with the breakdown curves indicates that the energy deposition peaks at ∼18 eV. This signifies that proton-naphthalene collisions at the 1 a.u. velocity regime also show the influence of plasmon (collective) excitation followed by autoionization and subsequent evaporation, similar to the case of photoionization of naphthalene. As the plasmon peaks between 13 and 19 eV, it is expected that a substantial fraction of plasmon-excited molecules should undergo evaporation after ionization. However, as the outgoing electron carries away some of the kinetic energy, the net energy available for subsequent dissociation is lower than the difference between plasmon energy and ionization potential.

IV. CONCLUSIONS

In contrast to many organic molecules, PAHs show resistance to fragmentation induced by radiation. The present work explores this mechanism through collisions between energetic protons and naphthalene. The mass spectrum includes narrow peaks corresponding to multiply ionized parent species or species with neutral fragment evaporation. The broader peaks are due to fragmentation of a multiply charged parent ion into charged fragments. H loss channel is observed to be the dominant evaporation channel followed by 2H loss. The ambiguity between 2H and H_2 is resolved by comparing mass spectra of previous measurements with PAHs. In the present case, this comparison shows that the evaporation process is sequential emission of neutral H. On the other hand, for double ionization, H_2 loss is observed to be an important pathway compared to H loss due to higher internal energy.

Unlike collisions with nucleobases (under identical conditions), naphthalene shows higher resilience for fragmentation and is observed with a charge state as high as 3+. Single and double ionization dominates over fragmentation yields. This is a very important observation considering that the nucleobases and naphthalene are similar in structure and composition as far as electronic stopping is concerned. A substantial fraction of dications are seen to decay via $2H/H_2$ loss or loss of C_2H_2, as opposed to single ionization in which the intact ion dominates over the loss of H and C_2H_2 species. Triple ionization, although present, is noted to have relatively low yield. The loss of $C_2H_2^+$ from dication is also observed in small fraction. However, the loss of H^+ from dication is conclusively absent. Therefore, for naphthalene dication, the threshold for loss of H^+ is less probable than that of $C_2H_2^+$. This is in agreement with the calculations by Holm *et al*. where the adiabatic dissociation energy for H^+ loss is twice that for $C_2H_2^+$ loss [27].

Measured relative cross sections show that ionization in the electron emission case dominates over the electron capture case by a factor of 3 in the studied velocity regime. In EE mode, the cross sections are found to be constant for single ionization. Evaporation channels, namely H, $2H/H_2$, and C_2H_2 loss, are observed to be independent of projectile velocity for both EE and EC modes in comparison to intact singly charged naphthalene. On the other hand, multifragmentation depends strongly on projectile velocity for EE mode, but is independent for EC mode.

Resonant and quasiresonant electron transfer model is invoked to explain the observed impact energy independence of evaporation as well as fragmentation channels with respect to intact single-ionization yield in the case of EC mode. The transfer condition is satisfied for several molecular orbitals inferred from DFT calculations performed for naphthalene. Comparing the recently published breakdown curves obtained with photoionization studies [68], we estimate that most of the EC events deposit energy between 6 and 10 eV. The excess energy, greater than 2 eV, is deposited by the electronic stopping of the projectile along with electron capture process.

In EE mode, while single-ionization cross sections show no observable dependence on the projectile velocity, multifragmentation depends strongly on projectile velocity. Consequently, two modes of energy transfer are implied: (i) a lower impact parameter process leading to mostly multifragmentation process and (ii) a larger impact parameter excitation process with energy transfer quantitatively similar to EC process. This is supported by the well-known collective excitation process in PAHs via photoionization measurements as well as ion-C_{60} collision studies. For C_{60}, it has been shown that plasmon or collective excitation process weakly depends on velocity but dominates the single- and double-ionization process in ion-C_{60} collisions. Thus, we conclude that for the single ionization of naphthalene, plasmon excitation has a significant influence.

ACKNOWLEDGMENTS

We thank IUAC staff for the smooth operation of the facility. Useful discussions with Professor Jens Ulrik Anderson and Professor Lokesh C. Tribedi are gratefully acknowledged.

[1] H. W. Jochims, E. Ruhl, H. Baumgartel, S. Tobita, and S. Leach, Int. J. Mass Spectrom. Ion Processes **167–168**, 35 (1997).

[2] I. V. Hertel, H. Steger, J. deVries, B. Weisser, C. Menzel, B. Kamke, and W. Kamke, Phys. Rev. Lett. **68**, 784 (1992).

[3] G. Portella, J. Poater, J. M. Bofill, P. Alemany, and M. Solá, J. Org. Chem. **70**, 2509 (2005).

[4] N. M. Marinov, W. J. Pitz, C. K. Westbrook, A. M. Vincitore, M. J. Castaldi, S. M. Senkan, and C. F. Melius, Combust. Flame **114**, 192 (1998).

[5] J. Appel, H. Bockhorn, and M. Frenklach, Combust. Flame **121**, 122 (2000).

[6] X. Wang, Y. Zhang, and R. F. Chen, Mar. Pollut. Bull. **42**, 1139 (2001).

[7] J. D. Bittner and J. B. Howard, Proc. Combust. Inst. **18**, 1105 (1981).

[8] A. G. G. M. Tielens, Annu. Rev. Astron. Astrophys. **46**, 289 (2008).

[9] M. Padovani, D. Galli, and A. E. Glassgold, Astron. Astrophys. **501**, 619 (2009).

[10] M. E. Wacks and V. H. Dibeler, J. Chem. Phys. **31**, 1557 (1959).

[11] R. J. Van Brunt and M. E. Wacks, J. Chem. Phys. **41**, 3195 (1964).

[12] H. Zettergren, H. T. Schmidt, P. Reinhed, H. Cederquist, Jens Jensen, P. Hvelplund, S. Tomita, B. Manil, J. Rangama, and B. A. Huber, J. Chem. Phys. **126**, 224303 (2007).

[13] H. Zettergren, H. T. Schmidt, P. Reinhed, H. Cederquist, J. Jensen, P. Hvelplund, S. Tomita, B. Manil, J. Rangama, and B. A. Huber, Phys. Rev. A **75**, 051201 (2007).

[14] W. Tappe, R. Flesch, E. Rühl, R. Hoekstra, and T. Schlathölter, Phys. Rev. Lett. **88**, 143401 (2002).

[15] T. Schlathölter, O. Hadjar, R. Hoekstra, and R. Morgenstern, Phys. Rev. Lett. **82**, 73 (1999).

[16] J. Postma, S. Bari, R. Hoekstra, A. G. G. M. Tielens, and T. Schlathölter, Astrophys. J. **708**, 435 (2010).

[17] H. A. B. Johansson, H. Zettergren, A. I. S. Holm, F. Seitz, H. T. Schmidt, P. Rousseau, A. Ławicki, M. Capron, A. Domaracka, E. Lattouf, S. Maclot, R. Maisonny, B. Manil, J.-Y. Chesnel, L. Adoui, B. A. Huber, and H. Cederquist, Phys. Rev. A **84**, 043201 (2011).

[18] A. Ławicki, A. I. S. Holm, P. Rousseau, M. Capron, R. Maisonny, S. Maclot, F. Seitz, H. A. B. Johansson, S. Rośen, H. T. Schmidt, H. Zettergren, B. Manil, L. Adoui, H. Cederquist, and B. A. Huber, Phys. Rev. A **83**, 022704 (2011).

[19] A. I. S. Holm, H. Zettergren, H. A. B. Johansson, F. Seitz, S. Rosén, H. T. Schmidt, A. Ławicki, J. Rangama, P. Rousseau, M. Capron, R. Maisonny, L. Adoui, A. Méry, B. Manil, B. A. Huber, and H. Cederquist, Phys. Rev. Lett. **105**, 213401 (2010).

[20] F. Seitz, A. I. S. Holm, H. Zettergren, H. A. B. Johansson, S. Rosén, H. T. Schmidt,A. Ławicki, J. Rangama, P. Rousseau, M. Capron, R. Maisonny, A. Domaracka, L. Adoui, A. Méry, B. Manil, B. A. Huber, and H. Cederquist, J. Chem. Phys. **135**, 064302 (2011).

[21] G. F. Bertsch, A. Bulgac, D. Tománek, and Y. Wang, Phys. Rev. Lett. **67**, 2690 (1991).

[22] Y. Ling and C. Lifshitz, Chem. Phys. Lett. **257**, 587 (1996).

[23] U. Kadhane, D. Misra, Y. P. Singh, and L. C. Tribedi, Phys. Rev. Lett. **90**, 093401 (2003).

[24] U. Kadhane, A. Kelkar, D. Misra, A. Kumar, and L. C. Tribedi, Phys. Rev. A **75**, 041201 (2007).

[25] Y. Gotkis, M. Oleinikova, M. Naor, and C. Lifshitz, J. Phys. Chem. **97**, 12282 (1993).

[26] E. Peeters, S. Hony, C. Van Kerckhoven, A. G. G. M. Tielens, L. J. Allamandola, D. M. Hudgins, and C. W. Bauschlicher, Astron. Astrophys. **390**, 1089 (2002).

[27] A. I. S. Holm, H. A. B. Johansson, H. Cederquist, and H. Zettergren, J. Chem. Phys. **134**, 044301 (2011).

[28] H. W. Jochim, E. Rühl, H. Baumgärtel, S. Tobita, and S. Leach, Astrophys. J. **420**, 307 (1994).

[29] A. Léger, P. Boissel, F. X. Désert, and L. d'Hendecourt, Astron. Astrophys. **213**, 351 (1989).

[30] M. H. Vuong and B. H. Foing, Astron. Astrophys. **363**, L5 (2000).

[31] L. J. Allamandola, A. G. G. M. Tielens, and J. R. Barker, Astrophys. J. **290**, L25 (1985).

[32] L. J. Allamandola, D. M. Hudgins, and S. A. Sandford, Astrophys. J. **511**, L115 (1999).

[33] A. Léger and J. L. Puget, Astron. Astrophys. **137**, L5 (1984).

[34] F. Salama, G. A. Galazutdinov, J. Krelowski, L. J. Allamandola, and F. A. Musaev, Astrophys. J. **526**, 265 (1999).

[35] F. Salama and L. J. Allamandola, Adv. Space Res. **15**, 413 (1995).

[36] G. C. Sloan, T. L. Hayward, L. J. Allamandola, J. D. Bregman, B. DeVito, and D. M. Hudgins, Astrophys. J. **513**, L65 (1999).

[37] E. L. O. Bakes and A. G. G. M. Tielens, Astrophys. J. **427**, 822 (1994).

[38] J. D. Thrower, B. Jørgensen, E. E. Friis, S. Baouche, V. Mennella, A. C. Luntz, M. Andersen, B. Hammer, and L. Hornekær, Astrophys. J. **752**, 3 (2012).

[39] M. Tarisien, L. Adoui, F. Frémont, D. Lelièvre, L. Guillaume, J.-Y. Chesnel, H. Zhang, A. Dubois, D. Mathur, S. Kumar, M. Krishnamurthy, and A. Cassimi, J. Phys. B: At. Mol. Opt. Phys. **33**, L11 (2000).

[40] J. G. Collins and P. Kebarle, J. Chem. Phys. **46**, 1082 (1967).

[41] J. M. Sanders, S. L. Varghese, C. H. Fleming, and G. A. Soosai, J. Phys. B: At. Mol. Opt. Phys. **36**, 3835 (2003).

[42] R. K. Janev, J. G. Wang, and T. Kato, in *Atomic and Plasma-Material Interaction Data for Fusion*, edited by R. E. H. Clark (International Atomic Energy Agency, Vienna, Austria, 2002),Vol. 10, pp. 129–149.

[43] B. Coupier, B. Farizon, M. Farizon, M. J. Gaillard, F. Gobet, N. V. de Castro Faria, G. Jalbert, S. Ouaskit, M. Carré, B. Gstir, G. Hanel, S. Denifl, L. Feketeova, P. Scheier, and T. D. Märk, Eur. Phys. J. D **20**, 459 (2002).

[44] J. Tabet, S. Eden, S. Feil, H. Abdoul-Carime, B. Farizon, M. Farizon, S. Ouaskit, and T. D. Märk, Phys. Rev. A **81**, 012711 (2010).

[45] J. Tabet, S. Eden, S. Feil, H. Abdoul-Carime, B. Farizon, M. Farizon, S. Ouaskit, and T. D. Märk, Phys. Rev. A **82**, 022703 (2010).

[46] M. E. Galassi, P. N. Abufager, P. D. Fainstein, and R. D. Rivarola, Phys. Rev. A **81**, 062713 (2010).

[47] A. L. F. de Barros, J. Lecointre, H. Luna, M. B. Shah, and E. C. Montenegro, Phys. Rev. A **80**, 012716 (2009).

[48] F. Gobet, B. Farizon, M. Farizon, M. J. Gaillard, M. Carre, M. Lezius, P. Scheier, and T. D. Mark, Phys. Rev. Lett. **86**, 3751 (2001).

[49] H. Lekadir, I. Abbas, C. Champion, O. Fojón, R. D. Rivarola, and J. Hanssen, Phys. Rev. A **79**, 062710 (2009).

[50] S. De, P. N. Ghosh, A. Roy, and C. P. Safvan, Nucl. Instrum. Methods Phys. Res., Sect. B **243**, 435 (2006).
[51] M. Krems, J. Zirbel, M. Thomason, and R. D. DuBois, Rev. Sci. Instrum. **76**, 093305 (2005).
[52] M. E. Rudd, R. D. DuBois, L. H. Toburen, C. A. Ratcliffe, and T. V. Goffe, Phys. Rev. A **28**, 3244 (1983).
[53] V. R. Bhardwaj, P. B. Corkum, and D. M. Rayner, Phys. Rev. Lett. **91**, 203004 (2003).
[54] M. E. Rudd, T. V. Goffe, and A. Itoh, Phys. Rev. A **32**, 2128 (1985).
[55] H. Tsuchida, A. Itoh, Y. Nakai, K. Miyabe, and N. Imanishi, J. Phys. B: At. Mol. Opt. Phys. **31** 5383 (1998).
[56] F. Gobet, S. Eden, B. Coupier, J. Tabet, B. Farizon, M. Farizon, M. J. Gaillard, M. Carré, S. Ouaskit, T. D. Märk, and P. Scheier, Phys. Rev. A **70**, 062716 (2004).
[57] N. Stolterforht, R. D. DuBois, and R. D. Rivarola, in *Electron Emission in Heavy Ion-Atom Collisions*, Springer Series on Atoms and Plasma, edited by G. Ecker, P. Lambropoulos, I. I. Sobel'man, and H. Walther (Springer, Berlin, 1997).
[58] N. Bohr and J. Lindhard, K. Dan. Vidensk. Selsk., Mat.-Fys. Medd. **28**, 7 (1954).
[59] A. Bárány, G. Astner, H. Cederquist, H. Danared, S. Huldt, P. Hvelplund, A. Johnson, H. Knudsen, L. Liljeby, and H.-G. Rensfelt, Nucl. Instrum. Methods Phys. Res., Sect. B **9**, 397 (1985).
[60] A. Long, J. Lu, A. Li, D. Hu, F. Liu, and Q. Zhang, J. Hazard. Mater. **150**, 656 (2008).
[61] A. O. Forsberg, J. D. Alexander, T. Chen, A. T. Pettersson, and M. Gatchell, J. Chem. Phys. **138**, 054306 (2013).
[62] H. Luna, A. L. F. de Barros, J. A. Wyer, S. W. J. Scully, J. Lecointre, P. M. Y. Garcia, G. M. Sigaud, A. C. F. Santos, V. Senthil, M. B. Shah, C. J. Latimer, and E. C. Montenegro, Phys. Rev. A **75**, 042711 (2007).
[63] F. Jolibois, A. Klotz, F. X. Gadéa, and C. Joblin, Astron. Astrophys. **444**, 629 (2005).
[64] P. Rousseau, A. Ławicki, A. I. S. Holm, M. Capron, R. Maisonny, S. Maclot, E. Lattouf, H. A. B. Johansson, F. Seitz, A. Méry, J. Rangama, H. Zettergren, S. Rosén, H. T. Schmidt, J.-Y. Chesnel, A. Domaracka, B. Manil, L. Adoui, H. Cederquist, and B. A. Huber, Nucl. Instr. Meth. Phys. Res. B **279**, 140 (2012).
[65] T. Allain, S. Leach, and E. Sedlmayr, Astron. Astrophys. **305**, 602 (1996).
[66] http://webbook.nist.gov/cgi/cbook.cgi?ID=C91203&Units=SI&Mask=20#Ion-Energetics, accessed on August 13, 2013.
[67] Y.-P. Ho, R. C. Dunbar, and C. Lifshitz, J. Am. Chem. Soc. **117**, 6504 (1995).
[68] B. West, C. Joblin, V. Blanchet, A. Bodi, B. Sztáray, and P. M. Mayer, J. Phys. Chem. A **116**, 10999 (2012).
[69] P. M. Mishra, J. Rajput, C. P. Safvan, S. Vig, and U. Kadhane (unpublished).
[70] S. Martin, L. Chen, R. Brédy, G. Montagne, C. Ortega, T. Schlathölter, G. Reitsma, and J. Bernard, Phys. Rev. A **85**, 052715 (2012).
[71] F. Alvarado, S. Bari, R. Hoekstra, and T. Schlathölter, J. Chem. Phys. **127**, 034301 (2007).
[72] M. J. Frisch, G. W. Trucks, H. B. Schlegel, G. E. Scuseria, M. A. Rob, J. R. Cheeseman, J. A. Montgomery, Jr., T. Vreven, K. N. Kudin, J. C. Burant, J. M. Millam, S. S. Iyengar, J. Tomasi, V. Barone, B. Mennucci, M. Cossi, G. Scalmani, N. Rega, G. A. Petersson, H. Nakatsuji *et al.*, *GAUSSIAN 03* (Gaussian, Inc., Wallingford, CT, 2003).